THE ASTROPHYSICAL JOURNAL, 341:190–200, 1989 June 1

CN AND CH VARIATIONS AMONG SUBGIANTS IN THE GLOBULAR CLUSTER 47 TUCANAE

GRAEME H. SMITH[1]
Space Telescope Science Institute

ROGER A. BELL
Astronomy Program, University of Maryland

AND

JAMES E. HESSER[1]
Dominion Astrophysical Observatory, Herzberg Institute of Astrophysics, National Research Council
Received 1988 April 6; accepted 1988 September 7

ABSTRACT

Observations of 28 giants and subgiants in the globular cluster 47 Tuc (NGC 104, Cl 0021-723) with absolute magnitudes in the range $+1 < M_v < +2$ have been obtained with the 2D-Frutti/RC-spectrograph combination on the CTIO 4 m telescope. This sample exhibits variations in the strength of the λ4215 CN band, which for the CN-richest subgiants anticorrelate with the strength of the λ4300 CH band. The present data, when considered in combination with published spectroscopy of bright giants and main-sequence turn-off stars, indicate that CN variations exist among stars in all stages of post–turn-off evolution in 47 Tuc.

Indices measuring the strength of the CN and CH bands have been derived from the spectra, and are compared with indices computed from synthetic spectra based on the model atmospheres computed using the MARCS program employed by Gustafsson *et al.* It is found that the λ4215 CN band strength of the CN-richest subgiants can be accounted for if it is assumed that the atmospheres of these stars were initially enhanced in nitrogen alone. It is difficult to match their CN band strengths by assuming that their atmospheres have been processed only through the CN-cycle of hydrogen burning, a significant amount of ON-processing seems also to be necessary. It is also shown that the pattern of C and N variations present among the 47 Tuc giants is dissimilar to that which would be expected from the type of progressive dredge-up of CN-processed material that is observed in M92 by Carbon *et al.* and Langer *et al.*

Subject headings: clusters: globular — stars: abundances — stars: late-type

I. INTRODUCTION

Being one of the most metal-rich and massive globular clusters in the Galaxy, 47 Tucanae has been a central object to the study of abundance variations within clusters. It was one of the first clusters found to be chemically inhomogeneous with regard to the elements carbon and nitrogen (Bell, Dickens, and Gustafsson 1975; Hesser, Hartwick, and McClure 1976, 1977; Hesser 1978; Mallia 1977, 1978; Norris 1978; Dickens, Bell, and Gustafsson 1979; Norris and Freeman 1979; Norris and Cottrell 1979; Hesser and Bell 1980; Bell, Hesser, and Cannon 1983; Norris, Freeman, and Da Costa 1984). Many of these studies have revealed that the brighter red giants in 47 Tuc with $M_v < +0.40$ exhibit noticeable differences in the strengths of the λ3883 and λ4215 CN bands and the λ4300 CH band. The distribution of λ4215 CN band strengths among these stars appears to be bimodal (Norris and Freeman 1979), with the CN-rich giants having weaker G bands, on average, than the CN-poor (Norris, Freeman, and Da Costa 1984). Similar CN and CH abundance variations have been discovered in the relatively advanced horizontal branch and asymptotic giant branch stages of evolution (Mallia 1978; Norris 1978; Norris and Freeman 1982). In addition, CN variations have been found to exist even among the main-sequence turn-off stars (Hesser 1978; Hesser and Bell 1980; Bell, Hesser, and Cannon 1983), a result which has important implications for the origin of these variations (Da Costa and Demarque 1982). Being of relatively high metal abundance, 47 Tuc is one of the few observationally accessible globular clusters in which the main-sequence turn-off stars are sufficiently cool that C and N abundance variations can produce observable variations in the strength of the λ3883 CN band. The observations of bright giant and main-sequence turn-off stars suggest that CN and CH variations exist throughout both the giant and subgiant branches.

It was with the aim of confirming this suggestion that a program of spectroscopy of 47 Tuc subgiants of intermediate luminosity has been carried out with the CTIO 4 m telescope. The present sample falls predominantly within the magnitude range $14.5 < V < 15.5$, i.e., $+1.1 < M_v < +2.1$ (using an apparent distance modulus of $[m - M_v] = 13.40$; Hesser *et al.* 1987), and complements the study by Norris and Freeman (1979) of a large sample of brighter stars having $-1.4 < M_v < +0.4$. The combined properties of the present data and those available in the literature should permit a conclusion as to whether CN variations are ubiquitous within 47 Tuc throughout all stages of post–main-sequence evolution.

II. OBSERVATIONS

Spectra were obtained of a sample of 28 subgiants in 47 Tucanae during the three nights of 1987 August 31 and September 1 and 2 with the 2D-Frutti detector on the RC spectrograph of the CTIO 4 m telescope. Program stars were selected from the color-magnitude diagram study of Hesser

[1] Visiting Astronomer, Cerro Tololo Inter-American Observatory, National Optical Astronomy Observatories, operated by the Association of Universities for Research in Astronomy, Inc., under contract with the National Science Foundation.

and Hartwick (1977), as well as from a list of stars for which CCD photometry was kindly provided by Dr. Alistair Walker. Two different spectrograph setups were used during the observing run. On the first night, grating 420 (600 lines mm^{-1}) was used in second-order blue with the Singer camera and a BG 38 filter to block first-order red light. On the second and third nights the first-order KPGL1 grating (632 lines mm^{-1} blazed at 4200 Å) was used without the BG 38. A 200 μm (1".5) wide slit was employed throughout the observing run; a slit length of 50" gave ample room on both sides of the program star spectrum from which to select appropriate windows for measuring the sky contribution. The wavelength range covered by the observations made on the first night was from 3670 Å to 4590 Å, at a scale along the dispersion direction of 0.6 Å pixel^{-1} and a FWHM resolution of ≈ 1.9 Å, while the range $\lambda\lambda$3670–5320 was observed on the second and third nights, at a scale on the detector of 1.1 Å pixel^{-1}, and a resolution of ≈ 4.6 Å.

Observations on the first two nights were made through occasional cloud, at least during the early parts of the night, and in seeing of $\approx 2''$–$3''$. The third night was completely clear with seeing of $\approx 1''$. Integration times per star generally ranged between 20 and 45 minutes, depending mainly on the seeing conditions, and the sky background, which was quite high during the first half of the nights due to a bright moon. Comparison HeNeAr lamp spectra were generally taken after each stellar integration. Flat-field exposures were obtained at the beginning of each night, and at two different grating angles, so as to optimize the counts in the blue and red sides of the detector. Integrations of 1 hr were taken for each of the red and blue settings per night. In addition, exposures of an incandescent lamp were obtained through a multihole decker each evening. This produced a series of continuous spectra across the 2D-Frutti image, the shapes of which were used to correct for the distortion of this instrument. Several flux standard stars were observed at the beginning and end of each night. Finally, 10,000 s dark exposures were obtained during the early morning hours following each night.

Data reduction was carried out both at the telescope during the night and day, and at the La Serena offices. All reductions employed the NOAO IRAF software package run on Sun workstations, and consisted of (1) summing all darks, smoothing them, and then subtracting them from the averaged flat-field exposures; (2) flat-fielding the raw data using the combined red and blue optimized flat fields for each night; (3) correction for distortion using fits to the loci of the multihole spectra; (4) extraction of raw one-dimensional spectra from each 2D-Frutti exposure of the 47 Tuc stars, together with sky subtraction, paying careful attention to the exclusion of light from any other star which happened to encroach upon the slit; (5) wavelength calibration of these one-dimensional spectra using a polynomial fit to the positions of lines in the HeNeAr arc spectra, followed by rebinning into equal λ-increment pixels; and (6) flux calibration of these rebinned spectra. It should be cautioned that because of the 1".5 slit width used, only limited confidence can be placed in the flux calibration achieved.

Upon obtaining the reduced spectra, the "splot" command in IRAF was used to compute the following spectroscopic indices, which provide a means of quantifying the strengths of the λ4215 CN and λ4300 CH molecular bands:

$$s_{\rm CN} = -2.5 \log_{10} (\bar{F}_{\lambda,\rm CN}/\bar{F}_{\lambda,\rm CP1}) ,$$

and

$$s_{\rm CH} = -2.5 \log_{10} (\bar{F}_{\lambda,\rm CH}/\bar{F}_{\lambda,\rm CP2}) ,$$

where $\bar{F}_\lambda$ refers to the mean flux per rebinned 2D-Frutti pixel over a specified wavelength range. The wavelength intervals used in computing these mean fluxes were $\lambda\lambda$4140–4220, $\lambda\lambda$4280–4320, and $\lambda\lambda$4220–4280 for $\bar{F}_{\lambda,\rm CN}$, $\bar{F}_{\lambda,\rm CH}$, and $\bar{F}_{\lambda,\rm CP1}$ respectively, while $\bar{F}_{\lambda,\rm CP2} = \frac{1}{2}(\bar{F}_{\lambda,\rm CP1} + \bar{F}_{\lambda,\rm CP3})$, where $\bar{F}_{\lambda,\rm CP3}$ is the mean flux in the bandpass $\lambda\lambda$4400–4480. These indices increase in value as the molecular absorption bands increase in strength. Three of the 47 Tuc program stars and several flux standards were observed on two or more nights. Although this does not provide a large set of repeated observations, the differences in the indices determined from these spectra can be used, together with the theory of small sample statistics, to estimate the present measurement errors. In this way, the standard deviation expected in a set of indices derived from single observations was calculated to be ≈ 0.02 for both $s_{\rm CN}$ and $s_{\rm CH}$. Given the small number of observations on which they are based, these error estimates should be viewed with caution.

The measured values of the CN and CH indices are listed in columns (5) and (6) of Table 1. The star designation in column (1) in most cases indicates the source of the V, $B-V$ photometry which is listed in columns (2) and (3). Stars denoted by a single prefix digit followed by a dash and four digits are identified in the paper of Hesser and Hartwick (1977); the number preceding the dash indicates the figure from their paper in which the stars are identified. The stars having designations of the form 5-*mnnn* are from Hesser and Hartwick's deep photographic study of the NE quadrant of 47 Tuc aimed at obtaining a complete luminosity function for the subgiant branch. The colors measured for these stars are expected to be the least accurate of those listed in Table 1; the reader is referred to Hesser and Hartwick (1977) for details. (The digit *m* in the above notation denotes one of the three sectors into which Hesser and Hartwick divide the NE quadrant). Stars which are included in the Walker CCD program, but not in that of Hesser and Hartwick (1977), are designated with the prefix AW. They are identified in the finding chart shown in Figure 1 (Plate 7) of the present paper. The source of the V, $B-V$ photometry for each star is given in column (4). The positions of the program stars in the color-magnitude diagram of 47 Tuc are shown in Figure 2, together with the fiducial sequences given by Hesser *et al.* (1987).

III. RESULTS

a) The CN *Variations*

A plot of the $s_{\rm CN}$ index versus V magnitude for the stars from Table 1 with $V > 13.8$ is shown in Figure 3. In the range $14.5 < V < 15.5$ a significant variation of the $s_{\rm CN}$ index is seen among stars of comparable magnitude. This range in $s_{\rm CN}$ of ~ 0.16 corresponds to an ≈ 5–8 σ variation, for $\sigma \approx 0.02$–0.03. Unlike the pattern seen among the bright giants (Norris and Freeman 1979), the present subgiant data show little or no evidence for a bimodal $s_{\rm CN}$ distribution. Figure 4 illustrates the CN variations further. It shows the spectra of stars 5-2466 and 5-3363, which are CN-poor, together with the spectra of 5-1620 and 5-3571, which are CN-rich. All four stars have V magnitudes of ≈ 15.05, but show a range of $s_{\rm CN}$ indices of ≈ 0.12. The CN enhancements among 5-1620 and 5-3571 are also exhibited by the λ3883 CN band, which is noticeably stronger among these two stars than among 5-2466 and 5-3363.

1989ApJ...341..190S

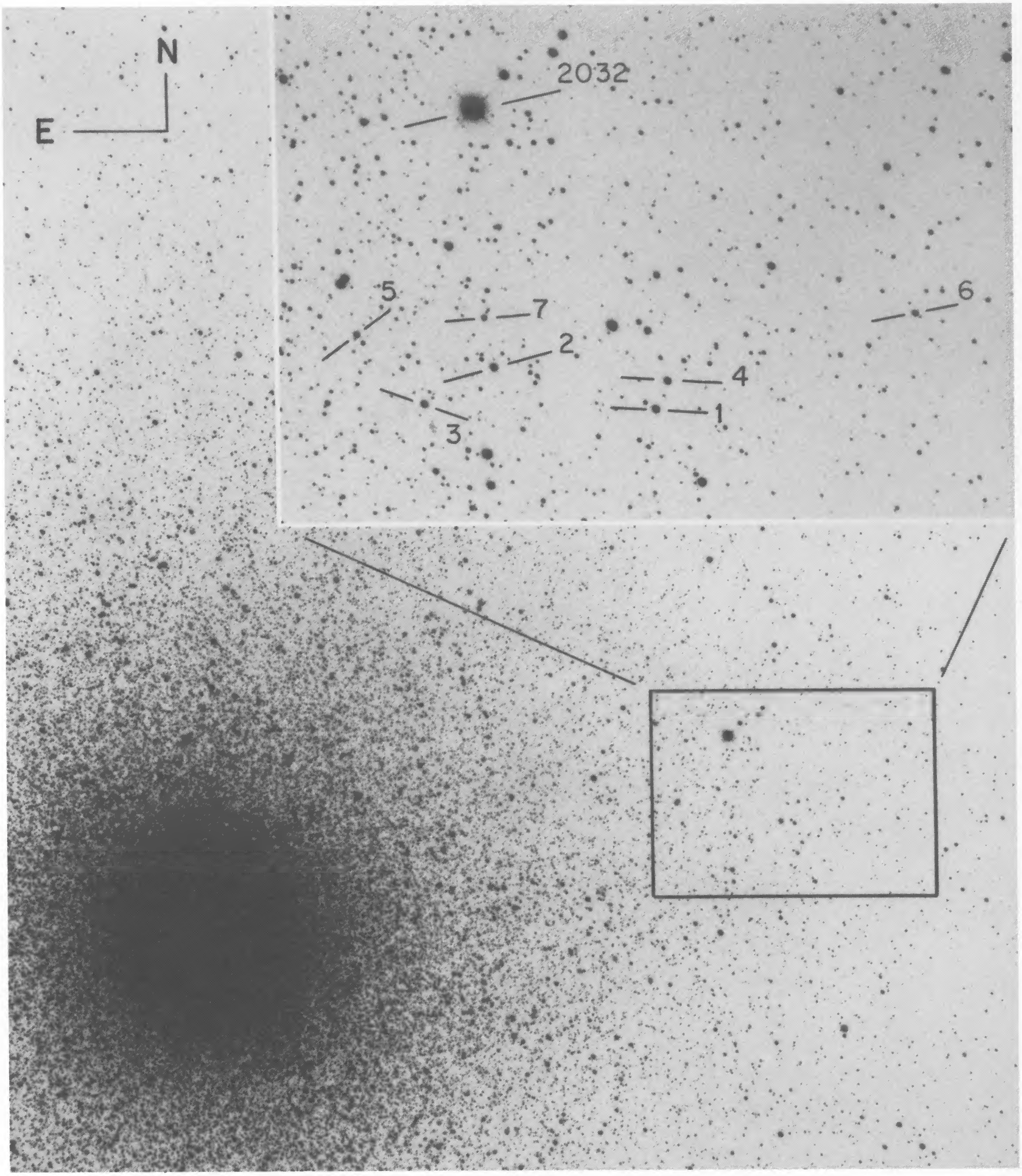

FIG. 1.—A finding chart for the seven stars in Table 1 that are identified with the prefix AW

SMITH, BELL, AND HESSLER (*see* **341**, 191)

TABLE 1

SPECTROSCOPIC INDICES FOR 47 TUCANAE SUBGIANTS

Star (1)	V (2)	$B-V$ (3)	Photometry Source (4)	s_{CN} (5)	s_{CH} (6)	δs_{CN} (7)
4-2005	13.197	1.125	AW	0.181	0.254	...
4-2102	13.29	1.13	HH	0.317	0.220	...
4-2082	13.96	0.95	HH	−0.010	0.280	−0.022
4-2106	14.10	0.96	HH	0.224	0.249	0.215
4-2151	14.22	0.96	HH	0.244	0.213	0.239
4-2177	14.37	0.93	HH	0.037	0.258	0.036
AW-1	14.585	0.918	AW	0.064	0.265	0.069
AW-2	14.590	0.928	AW	0.018	0.251	0.024
1-9038	14.615	0.901	AW	0.123	0.248	0.129
AW-3	14.817	0.854	AW	0.176	0.171	0.188
5-3344	14.93	0.89	HH	0.082	0.269	0.097
AW-4	14.944	0.902	AW	0.103	0.281	0.118
5-1528	14.98	0.85	HH	0.115	0.231	0.131
5-1620	15.01	0.87	HH	0.108	0.275	0.125
5-3348	15.03	0.89	HH	0.144	0.291	0.162
5-3363	15.03	0.88	HH	0.012	0.260	0.030
1-9016	15.037	0.91	AW	0.121	0.251	0.139
5-3571	15.06	0.88	HH	0.145	0.226	0.164
5-2466	15.06	0.81	HH	0.028	0.254	0.047
5-3380	15.10	0.85	HH	0.170	0.196	0.190
5-3307	15.17	0.90	HH	0.039	0.280	0.061
5-3375	15.22	0.82	HH	0.113	0.234	0.136
AW-5	15.379	0.832	AW	−0.038	0.266	−0.010
5-1527	15.38	0.81	HH	0.104	0.233	0.132
5-3310	15.38	0.87	HH	0.055	0.282	0.083
1-9015	15.493	0.868	AW	0.083	0.234	0.113
AW-6	15.617	0.819	AW	−0.053	0.266	−0.019
AW-7	15.967	0.815	AW	−0.057	0.244	−0.013

NOTE.—See text for explanation of cols. (1) and (4).

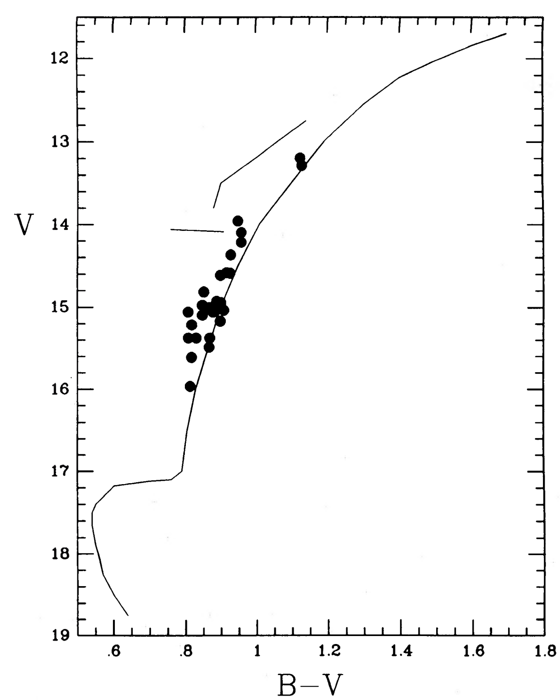

FIG. 2.—The V, $B-V$ color-magnitude diagram for the 47 Tuc subgiants observed in the present program (*closed circles*). The sources of the photometry are listed in Table 1. The fiducial locus of 47 Tuc is taken from Hesser *et al.* (1987).

b) The CH *Variations*

The G-band index s_{CH} is shown plotted against V in Figure 5. The range in this index among stars of comparable magnitude is much smaller than is the case with the CN index, most of the stars having s_{CH} values within a range of only ≈ 0.06, or ≈ 2–$3\ \sigma$. There do, however, appear to be several stars, such as AW-3 and 5-3380, which have noticeably weaker G bands than the others.

The relative behavior of the CN and CH indices is shown in Figure 6, where s_{CH} is plotted versus a CN-excess index δs_{CN} for stars with $V > 13.8$. The latter index is defined to be the displacement of each point in Figure 3 above a straight line having the equation $s_{CN} = -0.028V + 0.403$. This equation, which is shown in Figure 3, constitutes a reasonable baseline to the data, and was chosen to be an approximate fit to a locus computed from synthetic spectra for a giant branch appropriate to that of 47 Tuc and a solar ratio of C, N, and O to Fe (indices for these models are listed in group [A] of Table 2; see § IV below for details). As such, the baseline constitutes a locus of constant C and N abundance, and the index δs_{CN} is expected to be a reflection of the C and/or N abundance variations present among the subgiants. Among the bright giants, horizontal-branch stars, and asymptotic giant branch stars in 47 Tuc, Norris, Freeman, and Da Costa (1984), Norris and Freeman (1982), and Norris (1978), respectively, have found evidence that the G-band strength is anticorrelated with the $\lambda 4215$ or $\lambda 3883$ CN-band strength. This trend does appear to be evident in the present sample of stars, but only among those with the strongest CN bands, i.e., subgiants with $\delta s_{CN} > 0.13$ appear to have smaller s_{CH} indices than stars with $\delta s_{CN} < 0.13$. One star, 5-3348, appears to exhibit both strong CN and

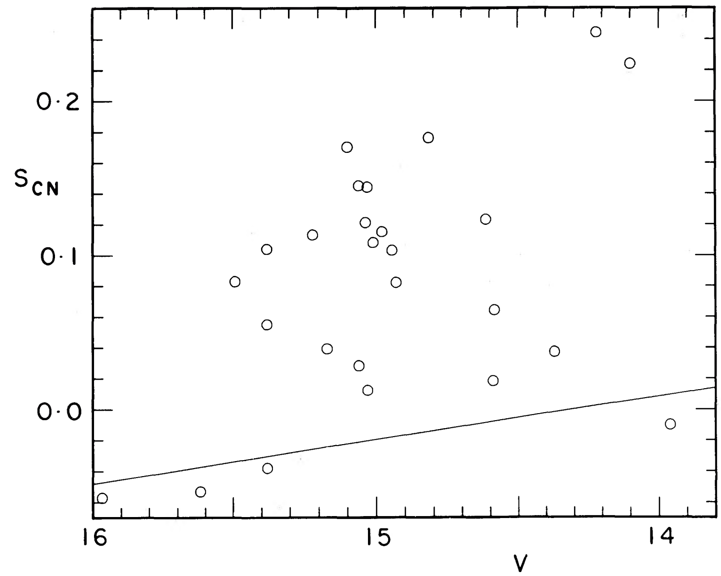

FIG. 3.—The λ4215 CN band strength index s_{CN} is shown plotted against V magnitude for the 47 Tuc subgiants listed in Table 1. A significant variation in s_{CN} is present among stars at all magnitude levels. The baseline relative to which the CN excess index δs_{CN} is measured is also shown.

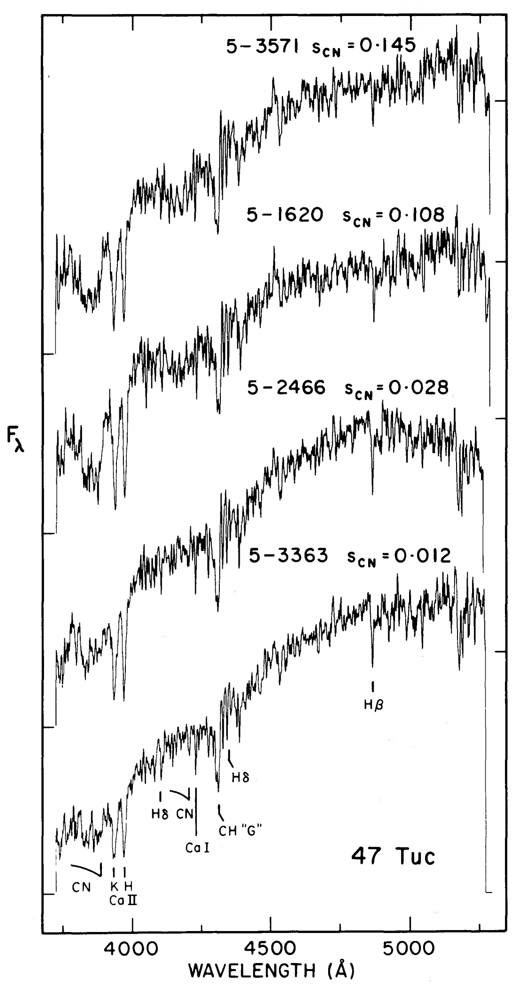

FIG. 4.—Spectra are shown for the four 47 Tuc subgiants 5-3571, 5-1620, 5-2466, and 5-3363. All four stars have similar V magnitudes and $B-V$ colors of ~ 15.05 and ~ 0.87, respectively. Despite their similar positions in the color-magnitude diagram, however, these stars exhibit noticeable differences in the strength of the λ4215 CN band. The value of the s_{CN} index is labeled next to each spectrum, the spectra being ordered from top to bottom in terms of decreasing CN band strength. Note that the two strongest λ4215 CN stars, 5-3571, and 5-1620, also display enhancements of the λ3883 CN band.

strong CH bands, although given that the present indices are derived from only one spectrum, this result should be confirmed by additional spectroscopy.

In summary, it appears that the 47 Tuc subgiants listed in Table 1 exhibit significant CN variations, but that only among the most CN-rich stars does the G band show an apparent decrease in strength. We now turn to an analysis of these data by a comparison with synthetic spectra.

IV. MODEL INDEX CALCULATIONS

In order to interpret the indices observed among the 47 Tuc stars, a series of s_{CN} and s_{CH} indices have been calculated for a grid of model stellar atmospheres appropriate to the giant branch of 47 Tuc. In order to do these calculations, it is first necessary to determine the run of temperature and surface gravity along the giant branch. The overall metal abundance adopted is $[A/H] = -0.8$ (Dickens, Bell, and Gustafsson 1979; Zinn and West 1984; Pilachowski 1984), and it is assumed initially that carbon, nitrogen, and oxygen are depleted by the same factor. The MARCS program (Gustafsson *et al.* 1975) was used to compute a number of flux constant, line-blanketed models for $[A/H] = -0.8$, the opacity distribution functions (ODFs) for these calculations being found by spline interpolation among ODFs computed for $[A/H] = 0.0$, -0.5, -1.0, and -2.0. The models were computed for a number of effective temperature values in the range 4000 K $\leq T_{eff} \leq$ 5000 K, and a set of surface gravities which was initially chosen on the basis of an earlier analysis of 47 Tuc stars by Dickens, Bell, and Gustafsson (1979). Synthetic

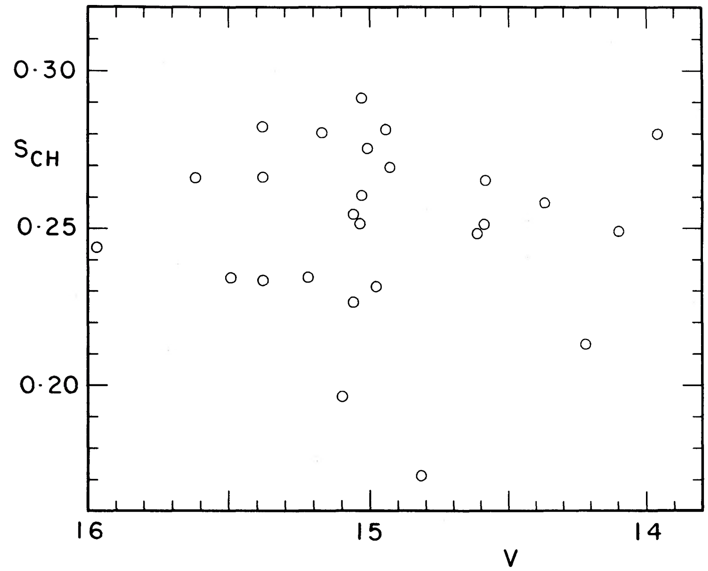

FIG. 5.—The λ4300 CH band index s_{CH} is plotted vs. V magnitude for the 47 Tuc subgiant sample from Table 1

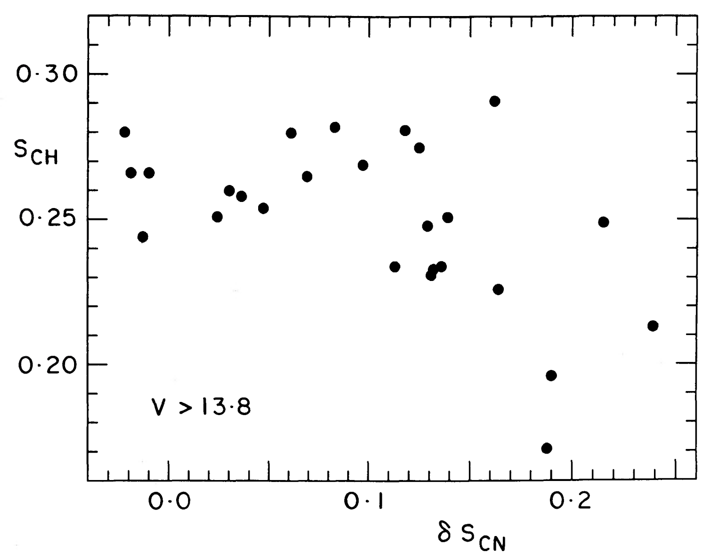

FIG. 6.—The s_{CH} index is plotted vs. the CN-excess index δs_{CN} for stars with $V > 13.8$

spectra were calculated for these models following Gustafsson and Bell (1979), using a resolution of 0.1 Å in the wavelength range 3000–12,000 Å and 1 Å in the wavelength range 9000–60,000 Å. A Doppler broadening velocity, including both thermal and turbulent terms, of 2 km s^{-1} was used for virtually all of the calculations. The absolute bolometric magnitude of the models is computed using

$$M_{\rm bol} = 4.72 - 2.5[m] + 2.5[g] - 10[T_{\rm eff}]\ ,$$

where m and g refer to the stellar mass and surface gravity. A mass of $m = 0.8\ M_\odot$ is adopted. The bolometric correction is found for each model from the relation

$$\mathrm{BC} = -2.5 \log\left(\int F_\lambda d\lambda \Big/ \int F_\lambda S_\lambda d\lambda\right) + \text{constant}\ ,$$

where F_λ is the model flux, and S_λ is the sensitivity function for the calculation of V magnitudes. The bolometric corrections are normalized to 0.07 mag for the Sun. The absolute visual magnitudes for the models are then found, and the models can be used to define lines of constant $T_{\rm eff}$ and log g in the V, $B-V$ color-magnitude diagram. The Hesser *et al.* (1987) fiducial points for the 47 Tuc color-magnitude diagram were corrected for a reddening of $E(B-V) = 0.03$, and the resulting V_0 values were converted to M_v using $V_0 - M_v = 13.3$. Comparison of these observed values with the model grid allows the run of surface gravity with temperature along the giant branch of 47 Tuc to be determined.

A set of models lying on or close to the 47 Tuc giant branch was chosen, the temperatures and surface gravities of which are recorded in Table 2, together with their V, M_v, and $M_{\rm bol}$ magnitudes, and $B-V$ color. A grid of s_{CN} and s_{CH} indices has been calculated for a range of input C, N, and O abundances for

TABLE 2

CN AND CH INDICES DERIVED FROM SYNTHETIC SPECTRA

T_{eff}	log g	[C/A]	[N/A]	[O/A]	V	$B-V$	s_{CN}	s_{CH}	BC	M_{bol}	M_v
					Group A						
4000............	1.25	...	...	...	12.80	1.230	0.022	0.273	−0.83	−1.43	−0.60
4250............	1.65	...	...	...	13.32	1.108	0.027	0.297	−0.62	−0.69	−0.08
4500............	2.25	...	...	...	14.43	0.967	−0.004	0.310	−0.47	0.56	1.03
4625............	2.50	...	...	...	14.88	0.910	−0.018	0.311	−0.42	1.07	1.48
4750............	2.70	...	...	...	15.22	0.859	−0.032	0.309	−0.37	1.45	1.82
4875............	3.20	...	...	...	16.32	0.809	−0.054	0.302	−0.33	2.59	2.92
5000............	3.65	...	...	...	17.41	0.767	−0.071	0.296	−0.30	3.60	3.91
					Group B						
4000............	1.25	−0.1	0.26	...	12.80	1.268	0.050	0.252	−0.83	−1.43	−0.60
4250............	1.65	−0.1	0.26	...	13.31	1.086	0.063	0.273	−0.60	−0.69	−0.09
4500............	2.25	−0.1	0.26	...	14.43	0.964	0.035	0.291	−0.47	0.56	1.03
4625............	2.50	−0.1	0.26	...	14.88	0.907	0.020	0.291	−0.42	1.07	1.48
4750............	2.70	−0.1	0.26	...	15.22	0.856	0.006	0.290	−0.37	1.45	1.82
4875............	3.20	−0.1	0.26	...	16.32	0.806	−0.021	0.283	−0.33	2.59	2.92
4000............	1.25	−0.3	0.49	...	12.80	1.259	0.053	0.219	−0.83	−1.43	−0.60
4250............	1.65	−0.3	0.49	...	13.32	1.094	0.072	0.242	−0.60	−0.69	−0.08
4500............	2.25	−0.3	0.49	...	14.43	0.954	0.049	0.254	−0.47	0.56	1.03
4625............	2.50	−0.3	0.49	...	14.88	0.897	0.038	0.255	−0.41	1.07	1.48
4750............	2.70	−0.3	0.49	...	15.21	0.846	0.026	0.253	−0.36	1.45	1.81
4875............	3.20	−0.3	0.49	...	16.32	0.796	0.001	0.243	−0.33	2.59	2.92
					Group C						
4000............	1.25	−0.2	0.61	−0.1	12.80	1.272	0.127	0.249	−0.83	−1.43	−0.60
4250............	1.65	−0.2	0.61	−0.1	13.30	1.090	0.166	0.269	−0.59	−0.69	−0.10
4500............	2.25	−0.2	0.61	−0.1	14.43	0.969	0.119	0.284	−0.47	0.56	1.03
4625............	2.50	−0.2	0.61	−0.1	14.88	0.912	0.101	0.283	−0.42	1.07	1.48
4750............	2.70	−0.2	0.61	−0.1	15.22	0.861	0.082	0.280	−0.37	1.45	1.82
4875............	3.20	−0.2	0.61	−0.1	16.32	0.810	0.044	0.272	−0.33	2.59	2.92
4000............	1.25	−0.3	0.76	−0.2	12.80	1.272	0.156	0.246	−0.83	−1.43	−0.60
4250............	1.65	−0.3	0.76	−0.2	13.30	1.088	0.198	0.262	−0.59	−0.69	−0.10
4500............	2.25	−0.3	0.76	−0.2	14.43	0.969	0.153	0.277	−0.47	0.56	1.03
4625............	2.50	−0.3	0.76	−0.2	14.88	0.912	0.134	0.275	−0.42	1.07	1.48
4750............	2.70	−0.3	0.76	−0.2	15.22	0.860	0.112	0.270	−0.37	1.45	1.82
4875............	3.20	−0.3	0.76	−0.2	16.32	0.809	0.072	0.261	−0.33	2.59	2.92
					Group D						
4000............	1.25	...	0.50	...	12.79	1.239	0.142	0.275	−0.82	−1.43	−0.61
4250............	1.65	...	0.50	...	13.30	1.090	0.166	0.296	−0.59	−0.69	−0.10
4625............	2.50	...	0.50	...	14.88	0.923	0.107	0.310	−0.42	1.07	1.48
4750............	2.70	...	0.50	...	15.22	0.871	0.085	0.308	−0.37	1.45	1.82
4875............	3.20	...	0.50	...	16.32	0.820	0.043	0.302	−0.33	2.59	2.92
					Group E						
4000............	1.25	−1.35	0.70	...	12.80	1.225	−0.035	0.094	−0.83	−1.43	−0.60
4250............	1.65	−1.08	0.68	...	13.32	1.061	0.006	0.128	−0.61	−0.69	−0.08
4625............	2.50	−0.68	0.63	...	14.88	0.876	0.019	0.186	−0.41	1.07	1.48
4750............	2.70	−0.51	0.59	...	15.22	0.835	0.022	0.213	−0.36	1.45	1.81
4875............	3.20	−0.36	0.52	...	16.32	0.793	0.001	0.232	−0.33	2.59	2.92

each of these models, and the results are also given in Table 2. The index calculations do not allow for any spectral smoothing due to the instrumental profile of a spectrograph. The models presented in this table are organized into five groups, each group corresponding to a different combination of C, N, and O abundances, several of which are thought to be representative of the effects that different types of mixing processes might have on the surface abundances of these elements. For group (A) it is assumed that the CNO elements are present in their solar abundance ratios (C = 8.62, N = 8.00, O = 8.86) depleted by the overall metal abundance of [A/H] = −0.8. The models in group (B) were calculated to simulate stars in which C → N processing has altered the atmospheric C and N abundances. The C abundance has been decreased by 0.1 and 0.3 dex, with the N being increased by 0.26 and 0.49 dex respectively (keeping C + N constant). As will be discussed below, the increases in the s_{CN} indices assuming only C → N processing are small relative to the observed variations. Further transformation of C into N will not significantly increase the strength of the CN band, since it is the abundance of C which is the limiting factor controlling the CN abundance. Consequently, a set of additional spectra, those in group (C) of Table 2, were computed allowing for both $C \rightarrow N$ and $O \rightarrow N$ processing. The relative amounts of these two processes are quite arbitrary; however, the resulting C abundance was kept less than the resulting O abundance in order to avoid producing carbon stars. In order to investigate the possible effects of a primordial variation in the abundance of N, the models in group (D) were computed with the N abundance enhanced by 0.5 dex. The models in group (E) are discussed below.

The results of these model index calculations are compared with the observations in Figures 7, 8, and 9. In Figure 7 the models from groups A, B, C, and D are plotted together with the data in the s_{CN} versus V diagram. The locus for solar CNO/Fe (*solid line*) provides quite a good baseline to the data, the s_{CN} indices for these models being comparable to the smallest indices observed among the 47 Tuc subgiants in the present sample. The locus for the group (B) models with a carbon depletion of [C/A] $= -0.3$ is shown in the figure as a long-dash, short-dash line. The predicted values of s_{CN} are near the maximum that can be obtained from $C \rightarrow N$ processing, but are still much smaller than the values observed among the CN-richest subgiants. It is concluded that $C \rightarrow N$ processing alone, in material initially having a solar C/N abundance ratio, cannot account for the CN indices of the CN-rich stars. The locus for models (C), with [C/A] $= -0.3$, [N/A] $= 0.76$, [O/A] $= -0.2$, do give stronger CN bands. The inclusion of $O \rightarrow N$ processing gives more N for a given C depletion, and also increases the amount of free carbon available for CN formation owing to the lesser amount of C locked up in CO formation. The s_{CN} indices are correspondingly larger. Although the present models in group (C) still do not match the largest s_{CN} values observed, it is expected that this could be accomplished with the addition of further arbitrary amounts of ON-processed material. It is concluded that if the CN-rich stars in 47 Tuc are assumed to owe their CN-enhancements to interior mixing, then the dredge-up of $O \rightarrow N$ processed material in addition to $C \rightarrow N$ material must be hypothesized.

The alternative to this hypothesis is the suggestion that 47 Tuc may have been inhomogeneously enriched in nitrogen by a primordial generation of stars more massive than those presently at the main-sequence turn-off. (Enrichment in carbon is not favored because it could lead to the production of carbon stars, and we observe no enhancement of the G band among the CN-rich stars.) The results for the models in group (D), with N enhancements of 0.5 dex, do in fact yield quite large s_{CN} values, and it can be seen from Figure 7 that an enhancement of $\Delta[N] \approx 0.7$–0.8 dex could probably account for the s_{CN} values of the CN-richest subgiants.

A comparison between the observed and model s_{CH} indices is shown in Figure 8, which is a plot of this CH band index versus V. In this case, the group (A) models form a locus which falls above the data, having s_{CH} values greater by ≈ 0.02 than the largest measured s_{CH} indices. This could be the result of systematic errors in either the observed s_{CH} indices, possibly due to an error in the flux calibration of the spectra, or the synthetic indices. Alternatively, the discrepancy may imply that carbon is slightly depleted relative to Fe and the other heavy elements among even the most CH-rich 47 Tuc subgiants. The models for [C/A] $= -0.1$, [N/A] $= 0.26$ give CH indices similar to those of the most CH-rich stars (the effect of the N enhancement on the CH band strength for these models is very small), suggesting the possibility that these stars may be depleted in carbon by ≈ 0.1 dex. Figure 8 also shows how the effect of a partial CNO-processing of an atmosphere is to produce a stronger G band than is attained by CN-processing to the same level of carbon depletion. As mentioned above, the depletion in oxygen accompanying CNO-processing leads to a greater free carbon abundance than is the case with material that has only been subjected to the CN-process. Neither the

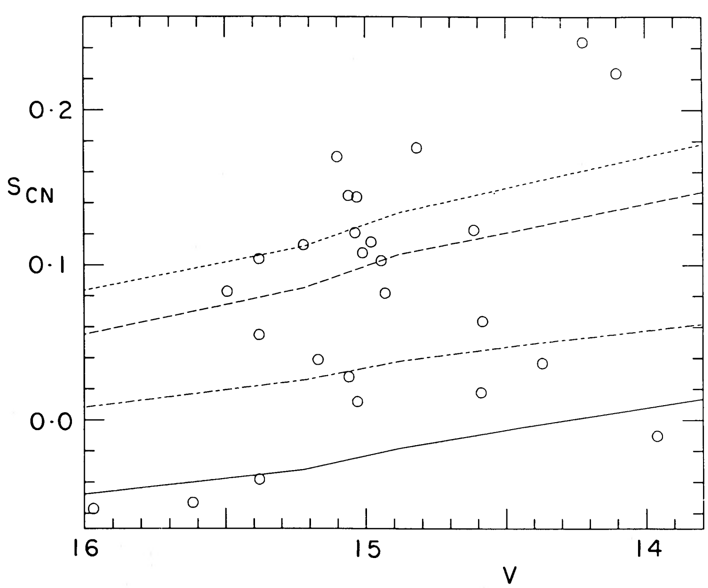

FIG. 7.—A plot of s_{CN} vs. V showing both the data from the present program, and the results of spectrum synthesis calculations. The observations are shown as open circles. Models for a simulated 47 Tuc giant branch with [CNO/Fe] $= 0$ are shown as a solid line. The group (D) models from Table 1 with [N/A] $= 0.5$, [C/A] $= 0$ are shown by the long-dash line; group (B) models with [C/A] $= -0.3$, [N/A] $= 0.49$ are depicted by a long-dash, short-dash line; while the group (C) models representative of $O \rightarrow N$ processing with [C/A] $= -0.3$, [N/A] $= 0.76$, and [O/A] $= -0.2$ are shown by a short-dash line. Of these models, only those with pure nitrogen enhancement or a contribution from ON-processing appear capable of producing a great enough s_{CN} increase relative to the solar CNO/Fe locus to be able to account for the CN enhancements of the CN-rich stars.

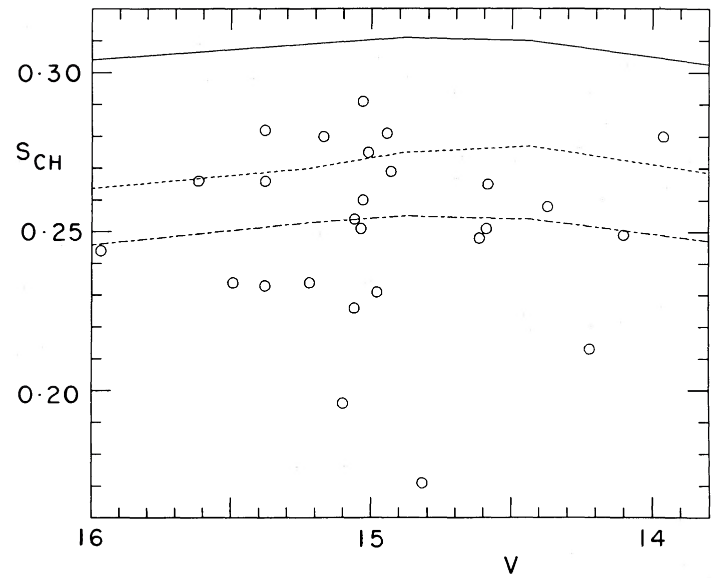

FIG. 8.—A comparison between observed and theoretical indices in the s_{CH} vs. V diagram. As in Fig. 7 different model sequences are depicted by different lines: solid line for [CNO/Fe] = 0; long-dash, short-dash for [C/A] = −0.3, [N/A] = 0.49; short-dash for [C/A] = −0.3, [N/A] = 0.76, [O/A] = −0.2.

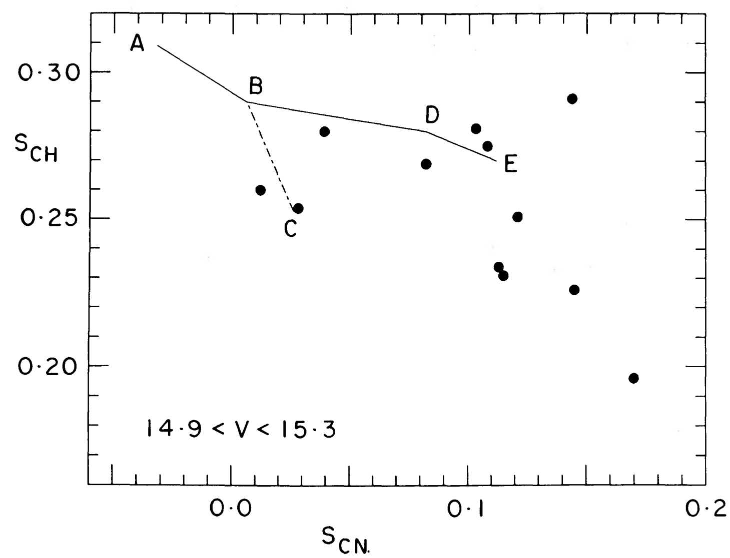

FIG. 9.—A plot of s_{CH} vs. s_{CN} for subgiants in the magnitude range $14.9 < V < 15.3$. Models for $V = 15.22$ from Table 2 are also shown; the dashed line shows the result for CN-processing alone where [C+N] = a constant, while the solid line shows the consequences of partial ON-processing. Models for five different abundance combinations are depicted in the figure; model A: [CNO/Fe] = 0; model B: [C/A] = −0.1, [N/A] = 0.26; model C: [C/A] = −0.3, [N/A] = 0.49; model D: [C/A] = −0.2, [N/A] = 0.61, [O/A] = −0.1; model E: [C/A] = −0.3, [N/A] = 0.76, [O/A] = −0.2.

C → N or O → N processed models depicted in Figure 8 reproduce the smallest G-band strengths observed among the CN-rich subgiants. To do so, it appears that carbon depletions of ≈0.5 dex or more may be necessary. In the presence of such low carbon abundances, it would again appear necessary to infer either a considerable degree of O → N processing, or a primordial nitrogen abundance enhancement, to account for the strong λ4215 CN bands of these stars, in agreement with the conclusions based on the s_{CN} data alone.

This result is further emphasized by Figure 9, in which the s_{CH} index is plotted against s_{CN} for stars in the restricted magnitude range $14.9 \le V \le 15.3$. The results for CN and CNO processed material, for models appropriate to $V = 15.22$ from Table 2, are also shown. Again, it can be seen that C → N processed material (represented by the curve ABC) is incapable of accounting for the strong CN bands observed. The ON-processed models (depicted by curve ABDE) do better, but a more extreme degree of processing than is assumed for the present models is needed to account for both the strong CN and weak CH bands of the most CN-rich subgiants.

The possible need for partial CNO-processing of the atmospheres of some 47 Tuc subgiants in order to explain their CN and CH variations suggests that a study of the 2.3 μm CO indices of 47 Tuc stars should be made. Indices for some bright giants have been published by Frogel, Persson, and Cohen (1981), and are shown versus $(V-K)_0$ in Figure 10. Stars are depicted as either filled or open circles depending on whether they were found to be CN-rich or CN-poor respectively by Norris and Freeman (1979). The CO indices for a number of models are given in Table 3. In addition to the calculations for solar [CNO/Fe] and CNO-processed material ([C/A] = −0.3, [N/A] = 0.76, [O/A] = −0.2), additional calculations were carried out adopting $^{12}C/^{13}C = 4$ instead of 89, and for a Doppler-broadening velocity of 3 km s^{-1} instead of 2 km s^{-1}. Since many of the CO lines are on the flat part of the curve of growth, this change has a very significant effect on the CO index. As discussed by Frogel, Persson, and Cohen (1981), the bright giants in 47 Tuc appear to show an anticorrelation between the λ4215 CN and 2.3 μm CO indices. Frogel, Persson, and Cohen attributed this anticorrelation to CN molecular line blocking of the comparison filter used in forming the CO index. To assess this possibility, models with N enhanced by 0.5 dex are also presented in Table 3. These models do exhibit a smaller CO index than models with solar [CNO/Fe] but only by $\approx$0.002–0.005, which is much smaller than the observed CO difference of $\approx$0.03 between the CN-rich and CN-poor giants. As a consequence, it is suggested that the observed CO, CN anticorrelation provides evidence for a C, N abundance anticorrelation between these stars. The model giant branches for [CNO/H] = [Fe/H] = −0.8, as well as for CNO-processed material, are shown in Figure 10. Although it might be argued that the curve for solar [CNO/Fe] is displaced upward by $\approx$0.01–0.02 relative to the mean CO indices for the CN-poor giants, the difference in CO between unmixed and CNO-processed models of similar $(V-K)_0$ color is comparable to that between the CN-poor and CN-rich giants. Furthermore, the C and O depletions used are arbitrary ones, and a better fit could be found by a more judicious choice. The hypothesis that O → N processed material has been mixed to the surface of the CN-rich 47 Tuc stars consequently appears to be supported by the available CO indices for the bright giants. Using photographic echelle spectra of the forbidden oxygen lines, Cottrell and Da Costa (1981) measured a difference of 0.1 dex in [O/Fe] abundance between two pairs of CN-rich and CN-poor red giants in 47 Tuc. This difference is small and may not be significant. Confirmation of this result with CCD spectroscopy would be very valuable.

TABLE 3

CO INDICES DERIVED FROM SYNTHETIC SPECTRA

T_{eff}	log g	[C/A]	[N/A]	[O/A]	$V-K$	CO
4000....	1.25	...	...	...	3.37	0.164
4250....	1.65	...	...	...	2.97	0.132
4500....	2.25	...	...	...	2.65	0.101
4750....	2.70	...	...	...	2.40	0.076
4000....	1.25	−0.3	0.76	−0.2	3.36	0.129
4250....	1.65	−0.3	0.76	−0.2	2.97	0.102
4500....	2.25	−0.3	0.76	−0.2	2.65	0.076
4750....	2.70	−0.3	0.76	−0.2	2.40	0.053
4000[a]...	1.25	...	...	...	3.36	0.215
4000[b]...	1.25	−0.3	0.76	−0.2	3.36	0.168
4250....	1.65	...	0.50	...	2.97	0.127
4500....	2.25	...	0.50	...	2.65	0.098
4750....	2.70	...	0.50	...	2.40	0.074

[a] DBV = 3.0 km s^{-1}.
[b] $^{12}C/^{13}C = 4$.

It is interesting to compare the pattern of CN variations observed in 47 Tuc with the strongly luminosity-dependent changes in carbon abundance found by Carbon *et al.* (1982) and Langer *et al.* (1986) in the metal-poor cluster M92 (see also Bell, Dickens, and Gustafsson 1979). Theoretical s_{CN} indices have been computed for a model 47 Tuc giant branch under

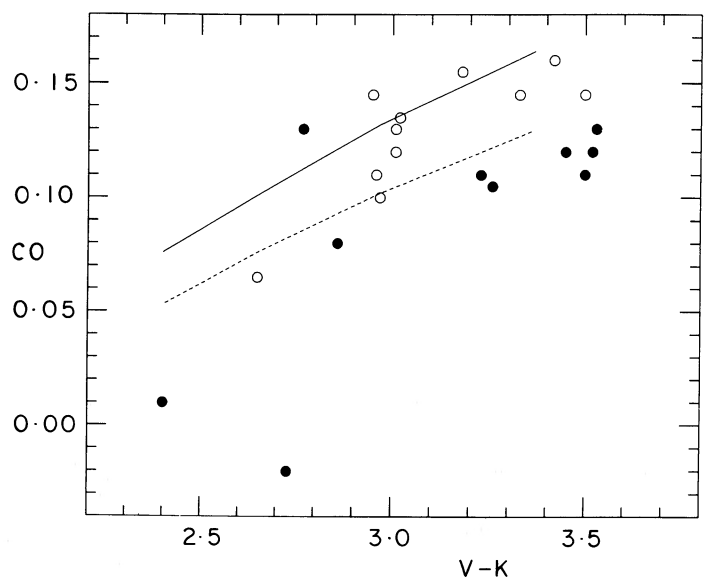

FIG. 10.—The infrared 2.3 μm CO index is plotted vs. $(V-K)_0$ for 47 Tuc red giants, the data being derived from Frogel *et al.* (1981). CN-rich giants are depicted by closed circles, CN-poor giants by open circles; the CN classifications being obtained from Norris and Freeman (1979). An anticorrelation between CO and CN is apparent. Model giant branches are shown for solar [CNO/Fe] (*solid line*), and [C/A] = −0.3, [N/A] = 0.76, [O/A] = −0.2 (*dashed line*).

the assumption that the carbon abundance declines with increasing luminosity at the rate of $\Delta[C/Fe]/\Delta V = 0.3$, which is similar to the decline observed among the M92 giants by Carbon *et al.* and Langer *et al.* Mixing is assumed to start at the base of the subgiant branch at $V = 17.4$, and the depleted ^{12}C is taken to be converted entirely to ^{14}N. The theoretical s_{CN} indices computed as a function of V magnitude are shown in Figure 11. Relative to a giant branch in which [C/Fe] = [N/Fe] = 0 at all luminosities (*solid line*), the CN indices in the case of progressive mixing (*dashed line*) reach a maximum enhancement of $\Delta s_{CN} \approx 0.07$ in the magnitude range $V = 15.0$–16.0. A turnover in the CN abundance is produced, which results from the fact that in heavily CN-processed material the nitrogen abundance attains an approximately constant value, so that a progressively decreasing C abundance will produce a progressively decreasing CN abundance (Smith and Bell 1986; Smith 1987). The maximum difference of ≈ 0.07 in s_{CN} between mixed and unmixed models, is much less than the range of ≈ 0.16 observed among the 47 Tuc subgiants of magnitude $V \sim 15$. This comparison again emphasizes the inability of $C \rightarrow N$ processing alone to account for the observations. Notice also that progressive mixing would produce CN-weak stars on the upper red giant branch, not CN-rich stars. The fact that CN band enhancements exist among the bright 47 Tuc giants, as documented in the papers cited in the Introduction, implies that the 47 Tuc stars are not undergoing an extreme type of progressive giant branch mixing such as is seen in M92. This point has been discussed by Bell and Dickens (1980; see also the review by Norris 1988). The low carbon abundances that would be produced among the 47 Tuc red giants by progressive mixing are inconsistent with the near-solar [C/Fe] abundances observed among these stars by Dickens, Bell, and Gustafsson (1979).

V. CONCLUSIONS

The observations reported in this paper show that variations in the strength of the λ4215 CN band exist among 47 Tuc subgiants having absolute magnitudes in the range $+1.1 < M_v < +2.1$. The most CN-rich stars ($\delta s_{CN} > 0.13$) exhibit weaker CH bands than the most CN-poor, although among the majority of stars with $\delta s_{CN} < 0.13$ the present data reveal no significant evidence of G-band variations. These results, when considered together with the spectroscopy of Hesser (1978), Norris and Freeman (1979), and Norris, Freeman, and Da Costa (1984) for the bright giants, and Hesser (1978), Hesser and Bell (1980), and Bell, Hesser, and Cannon (1983) for the main-sequence turn-off stars, demonstrate that CN variations are prevalent throughout the entire giant branch. The dredge-up of CN-processed material alone does not appear capable of explaining the range in s_{CN} values observed among the 47 Tuc subgiants. Unless interior mixing is able to access ON-processed material, a theory involving primordial nitrogen enrichment may be required.

The present observations imply that any hypothetical dredge-up of ON-processed material must have occurred within stars having an absolute magnitude fainter than $M_v \sim +2.0$, while the observations of Hesser (1978), Hesser and Bell (1980), and Bell, Hesser, and Cannon (1983), as well as unpublished AAT observations by the same authors, show that CN variations are present among main-sequence turn-off stars, thereby indicating that they are the products of events which occurred during an even earlier evolutionary phase. VandenBerg and Smith (1988) found no satisfactory site for a deep mixing event prior to the main-sequence turn-off, apart from the pre–main-sequence and early–main-sequence phases when the star is still largely homogeneous (see also Da Costa and Demarque 1982). Some interior $C \rightarrow N$ processing does take place during these early evolutionary phases, so that accompanying deep-mixing could change the surface C and N abundances without radically altering the subsequent evolutionary track. However, even this possibility is challenged by the present observations, which would require $O \rightarrow N$–processed

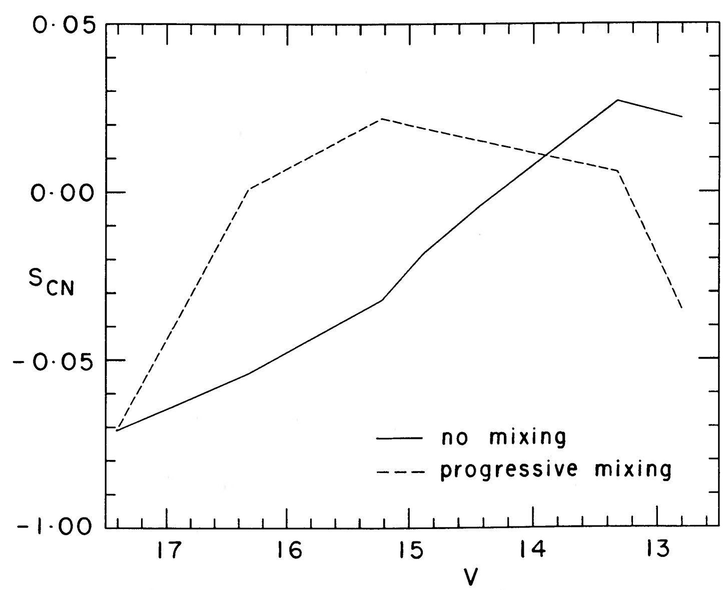

FIG. 11.—The variation of s_{CN} as a function of V is computed for a simulated 47 Tuc giant branch and two different assumptions regarding the behavior of the C abundance as a function of stellar luminosity. The solid line shows the case in which the C abundance is kept constant at [C/Fe] = 0, [Fe/H] = −0.8. The dashed line shows the consequences of assuming that the C abundance declines with increasing luminosity at the rate $\Delta[C/Fe]/\Delta V = 0.3$, with nitrogen increasing accordingly so as to keep C + N constant (see the models from group E in Table 2).

material to be present at the surface of a CN-rich 47 Tuc subgiant. The models for a star of mass 0.8 $M_\odot$, $Y = 0.20$, and $Z = 10^{-4}$ discussed by Sneden, Pilachowski, and VandenBerg (1986) show that at least up to an age of 9×10^9 yr on the main-sequence no ON-processing has taken place within the stellar interior. Pre–main-sequence or early–main-sequence mixing of low-mass globular cluster stars is therefore not expected to dredge up ON-processed material, and therefore appears not to explain the observational results.

It would be very valuable to use CCD spectrographs to follow up the work of Cottrell and Da Costa (1981) by determining oxygen abundances for CN-rich and CN-poor red giants in 47 Tuc, in order to constrain the possibility that ON-processed material is present in the atmospheres of the CN-rich stars.

Although the origin of the CN variations in 47 Tuc remains elusive, the observations may nonetheless provide some information about stellar interior mixing as a function of metallicity. Luminosity-dependent dredge-up of CN-processed material of the type observed among the stars in the metal-poor clusters M92 and M15 (Carbon *et al.* 1982; Trefzger *et al.* 1983; Langer *et al.* 1986) is calculated to produce CN-poor, and not CN-rich, stars on the upper giant branch. The presence of many CN-rich giants in 47 Tuc and other clusters such as NGC 6352 (Hesser, Hartwick, and McClure 1977), NGC 6752 (Norris *et al.* 1981), M4 (Norris 1981), and M5 (Smith and Norris 1983), suggests the lack of such mixing within cluster giants of intermediate to relatively-high metal abundance. This suggestion is consistent with the finding by Bell and Dickens (1980) that the [C/Fe] abundance of bright cluster giants correlates with their [Fe/H] metallicity. One reason why interior mixing within red giants might be dependent on metal abundance has been explored by Sweigart and Mengel (1979), who showed that within such stars, the extent of regions of C $\rightarrow$ N and O $\rightarrow$ N processing beyond the hydrogen-burning shell varies with the metal abundance, being greatest for the most metal-poor giants. Thus it may be that these stars experience the most favorable conditions for the dredge-up of CNO-processed material.

We wish to thank the staff of CTIO for their support during the observing run on which the present data were obtained. In particular, we thank Mario Hamuy and Mauricio Navarrete for their invaluable assistance with the data reduction. We thank Alistair Walker for providing photometry and finding charts for seven of our program stars. We are grateful for computing assistance from Michael Briley and J. T. Ohlmacher at the University of Maryland. Part of this work was supported by the National Science Foundation, under grant AST85-13872. The spectrum synthesis calculations were made using the Cray X-MP of the San Diego Supercomputer Center, the time being supplied under NSF grant AST85-09915. The interpretation of the results was materially assisted by the use of a Ridge 32C computer and Chromatics CX-1536 image display system, purchased under the above grants.

REFERENCES

Bell, R. A., and Dickens, R. J. 1980, *Ap. J.*, **242**, 657.
Bell, R. A., Dickens, R. J., and Gustafsson, B. 1975, *Bull. AAS*, **7**, 535.
———. 1979, *Ap. J.*, **229**, 604.
Bell, R. A., Hesser, J. E., and Cannon, R. D. 1983, *Ap. J.*, **269**, 580.
Carbon, D. F., Langer, G. E., Butler, D., Kraft, R. P., Suntzeff, N. B., Kemper, E., Trefzger, C. F., and Romanishin, W. 1982, *Ap. J. Suppl.*, **49**, 207.
Cottrell, P. L., and Da Costa, G. S. 1981, *Ap. J. (Letters)*, **245**, L79.
Da Costa, G. S., and Demarque, P. 1982, *Ap. J.*, **259**, 193.
Dickens, R. J., Bell, R. A., and Gustafsson, B. 1979, *Ap. J.*, **232**, 428.
Frogel, J. A., Persson, S. E., and Cohen, J. G. 1981, *Ap. J.*, **246**, 842.
Gustafsson, B., and Bell, R. A. 1979, *Astr. Ap.*, **74**, 313.
Gustafsson, B., Bell, R. A., Eriksson, K., and Nordlund, Å. 1975, *Astr. Ap.*, **42**, 407.
Hesser, J. E. 1978, *Ap. J. (Letters)*, **223**, L117.
Hesser, J. E., and Bell, R. A. 1980, *Ap. J. (Letters)*, **238**, L149.
Hesser, J. E., Harris, W. E., VandenBerg, D. A., Allwright, J. W. B., Shott, P., and Stetson, P. B. 1987, *Pub. A.S.P.*, **99**, 739.
Hesser, J. E., and Hartwick, F. D. A. 1977, *Ap. J. Suppl.*, **33**, 361.
Hesser, J. E., Hartwick, F. D. A., and McClure, R. D. 1976, *Ap. J. (Letters)*, **207**, L113.
———. 1977, *Ap. J. Suppl.*, **33**, 471.
Langer, G. E., Kraft, R. P., Carbon, D. F., Friel, E., and Oke, J. B. 1986, *Pub. A.S.P.*, **98**, 473.
Mallia, E. A. 1977, *Astr. Ap.*, **60**, 195.
Mallia, E. A. 1978, *Astr. Ap.*, **70**, 115.
Norris, J. 1978, in *IAU Symposium 80, The H-R Diagram*, ed. A. G. Davis Philip and D. S. Hayes (Dordrecht: Reidel), p. 195.
———. 1981, *Ap. J.*, **248**, 177.
———. 1988, in *IAU Symposium 126, The Harlow-Shapley Symposium on Globular Cluster Systems in Galaxies*, ed. J. E. Grindlay and A. G. Davis Philip (Dordrecht: Reidel), p. 93.
Norris, J., and Cottrell, P. L. 1979, *Ap. J. (Letters)*, **229**, L69.
Norris, J., Cottrell, P. L., Freeman, K. C., and Da Costa, G. S. 1981, *Ap. J.*, **244**, 205.
Norris, J., and Freeman, K. C. 1979, *Ap. J. (Letters)*, **230**, L179.
———. 1982, *Ap. J.*, **254**, 143.
Norris, J., Freeman, K. C., and Da Costa, G. S. 1984, *Ap. J.*, **277**, 615.
Pilachowski, C. A. 1984, *Ap. J.*, **281**, 614.
Smith, G. H. 1987, *Pub. A.S.P.*, **99**, 67.
Smith, G. H., and Bell, R. A. 1986, *A.J.*, **91**, 1121.
Smith, G. H., and Norris, J. 1983, *Ap. J.*, **264**, 215.
Sneden, C., Pilachowski, C. A., and VandenBerg, D. A. 1986, *Ap. J.*, **311**, 826.
Sweigart, A. V., and Mengel, J. G. 1979, *Ap. J.*, **229**, 624.
Trefzger, C. F., Carbon, D. F., Langer, G. E., Suntzeff, N. B., and Kraft, R. P. 1983, *Ap. J.*, **266**, 144.
VandenBerg, D. A., and Smith, G. H. 1988, *Pub. A.S.P.*, **100**, 314.
Zinn, R., and West, M. J. 1984, *Ap. J. Suppl.*, **55**, 45.

ROGER A. BELL: Astronomy Program, University of Maryland, College Park, MD 20742

JAMES E. HESSER: Dominion Astrophysical Observatory, Herzberg Institute of Astrophysics, 5071 West Saanich Road, Victoria, British Columbia, Canada V8X 4M6

GRAEME H. SMITH: Space Telescope Science Institute, 3700 San Martin Drive, Baltimore, MD 21218